# Functional Role of Second Heart Field-derived Smooth Muscle Cells in Thoracic Aortopathies in Mice

Hisashi Sawada[1], Hideyuki Higashi[2], Chen Zhang[3, 4], Yanming Li[3, 4], Yuriko Katsumata[5], Stephanie Morgan[2], Lang H. Lee[2], Sasha A. Singh[2], Jeff Z. Chen[1, 6], Jessica J. Moorleghen[1], Deborah A. Howatt[1], Debra L. Rateri[1], Hong S. Lu[1, 6], Ying H. Shen[3, 4], Scott A. LeMaire[3, 4], Masanori Aikawa[2], Mark W. Majesky[7], Alan Daugherty[1, 6]

1. Saha Cardiovascular Research Center, University of Kentucky, KY
2. Center for Interdisciplinary Cardiovascular Sciences, Cardiovascular Division, Department of Medicine, Brigham and Women's Hospital, Harvard Medical School, Boston, MA
3. Division of Cardiothoracic Surgery, Michael E. DeBakey Department of Surgery, Baylor College of Medicine, Houston, TX
4. Department of Cardiovascular Surgery, Texas Heart Institute, Houston, TX
5. Department of Biostatistics, University of Kentucky, KY
6. Department of Physiology, University of Kentucky, KY
7. Center for Developmental Biology & Regenerative Medicine, Seattle Children's Research Institute, Departments of Pediatrics and Pathology, University of Washington, Seattle, WA

**Running title:** SHF-derived SMCs impact TAA

**Corresponding author:**

Alan Daugherty

Saha Cardiovascular Research Center, University of Kentucky

741 South Limestone Street

BBSRB, B243

Lexington, KY, 40536, USA.

Tel: +1-859-323-3512

E-mail: alan.daugherty@uky.edu

**Word count:**

Abstract: 350 words

Manuscript: 3,684 words

**Abstract**

**Background:** The ascending aorta is a common location for thoracic aortopathies. Pathology predominates in the aortic media with disease severity being most apparent in outer laminar layers. In the ascending aorta, smooth muscle cells (SMCs) are derived from two embryonic origins: cardiac neural crest and second heart field (SHF). SMCs of these origins have distinct distributions, and the localization of SHF coincides with the regional specificity in some forms of thoracic aortopathies. However, the role of SHF-derived SMCs in maintaining the structural and functional integrity of the ascending aorta remains unclear.

**Methods:** Mass spectrometry assisted proteomic and single cell transcriptomic analyses were performed in mouse aortas to discriminate molecular features of SHF-derived SMCs in maintaining the aortic homeostasis. Genetic deletion of low-density lipoprotein receptor-related protein 1 (*Lrp1*) or transforming growth factor-β receptor 2 (*Tgfbr2*) in SHF-derived SMCs was conducted to examine impact of SHF-derived SMCs on the development of thoracic aortopathies.

**Results:** Proteomic analysis did not detect differences in protein profiles between ascending (disease prone) and descending (disease resistant) thoracic aortas in saline-infused mice. However, angiotensin II infusion altered these profiles in a region-specific manner. Angiotensin II evoked differential expression of multiple LRP1 ligands. Histological analysis demonstrated that angiotensin II-induced medial disruptions were detected mainly in outer laminar layers derived from the SHF. Single cell RNA sequencing using normal mouse aortas revealed lower abundance of elastin mRNA in SHF-derived SMCs compared to SMCs from the cardiac neural crest. In addition, *Lrp1*

and *Tgfbr2* mRNA were abundant in SHF-derived SMCs. To examine biological effects of SHF-derived cells, *Lrp1* or *Tgfbr2* was deleted in SHF-derived cells in mice. SHF-specific *Lrp1* deletion augmented angiotensin II-induced aortic aneurysm and rupture in the ascending region. Proteomic analysis discerned regulation of protein abundances related to TGF-β signaling pathways by *Lrp1* deletion in SHF-derived cells. Deletion of *Tgfbr2*, a key regulator of TGF-β signaling, in SHF-derived cells led to embryonic lethality at E12.5 with dilatation of the outflow tract and retroperitoneal hemorrhage in mice.

**Conclusion:** These results demonstrate that SMCs derived from the SHF play a critical role in the integrity of the ascending aortic wall.

## Introduction

Thoracic aortopathies are a spectrum of lethal diseases associated with aneurysms, dissection, and rupture.[1, 2] Despite the devastating consequences of these diseases, current medical therapy has limited efficacy. Therefore, there is an urgent need to investigate mechanisms of thoracic aortopathies to facilitate development of novel therapeutics.

Aortopathies occur throughout the thoracic aorta with the ascending aortic segment being a frequently affected region.[3, 4] Medial thickening is a histological feature of thoracic aortopathies, and this pathology shows a gradient across the media that is detected predominantly in outer laminar layers.[5-10] Therefore, thoracic aortopathies have regional and transmural specificities with outer medial layers in the ascending aorta being a disease-prone location. However, the mechanism by which outer medial layers of the ascending aorta are prone to aortopathy remains unclear.

The major cellular component of the aortic media is smooth muscle cells (SMCs), and these cells exert a pivotal role in the pathogenesis of thoracic aortopathies.[11] SMCs in the ascending aorta are derived from two different embryonic origins: cardiac neural crest (CNC) and second heart field (SHF).[12] Although it is not possible to grossly discern the origin of aortic SMCs, lineage tracking studies have demonstrated that CNC-and SHF-derived SMCs occupy inner and outer layers, respectively, of the ascending aorta.[13] The region-specific distribution of thoracic aortopathies appears to coincide with the distribution of SMCs from the SHF rather than CNC. Thus, differences of embryonic origins may lead to functional differences that have pathological consequences. However, there is scant evidence supporting this hypothesis. In this

study, we investigated whether SMCs derived from the SHF colocalized with the evolution of aortic pathology produced by chronic angiotensin II (AngII) infusion in mice,[6, 14, 15] and investigated the molecular basis for the regional specificity of thoracic aortopathies using a proteomic and single cell transcriptomic approaches. The omics studies identified low-density lipoprotein receptor-related protein 1 (*Lrp1*) and transforming growth factor (TGF)-β receptor 2 (*Tgfbr2*) as potential targets. SHF-specific deletion of either *Lrp1* or *Tgfbr2* gene was then performed to investigate the effects of SHF-derived SMCs on development of thoracic aortopathies.

## Methods

Additional detailed methods are presented in **Supplemental Methods**. All raw data and analytical methods are available from the corresponding author upon appropriate request.

*Mice*

The following mice were purchased from The Jackson Laboratory (**Supplemental Table I**): ROSA26R$^{LacZ}$ (#003474), ROSA26R$^{mT/mG}$ (#007676), *Lrp1* floxed (#012604), *Tgfbr2* floxed (#012603), Wnt1-*Cre* [#022501 (C57BL/6J background, also known as B6-Wnt1-*Cre*2), #022137 (Wnt1-*Cre*2 on a 129S4 background)]. Mef2c-*Cre* mice (#030262) were purchased from the Mutant Mouse Resource and Research Center. For cell tracking studies of CNC and SHF origins, either Wnt1-*Cre* (#022501) or Mef2c-*Cre* male mice were bred to ROSA26R$^{LacZ}$ female mice, respectively. For the single cell RNA sequence study, Mef2c-*Cre* male mice were bred to ROSA26R$^{mT/mG}$ female mice. To delete LRP1 in CNC-derived cells, Wnt1-*Cre* mice were bred with *Lrp1* floxed female mice. Embryonic lethality, a phenotype of LRP1 deletion in CNC-derived cells, was confirmed using the 129S4 background Wnt1-*Cre* strain. Embryos with CNC-specific LRP1-deletion were harvested from *Lrp1* floxed female mice bred with Wnt1-*Cre* (#22137) males. To delete LRP1 in SHF-derived cells, Mef2c-*Cre* male mice were crossbred to *Lrp1* floxed female. Wnt1-*Cre* and Mef2c-*Cre* male mice were used for lineage-specific deletion of TGFBR2 in CNC and SHF-derived cells, respectively. Because of the low incidence of AngII-induced thoracic aortic aneurysms (TAAs) in female mice, only male mice were studied.[16] All experiments were approved by the IACUC at the University of Kentucky or Baylor College of Medicine in accordance with

the guidelines of the National Institutes of Health.

*Pump implantation*

After random assignment, saline or AngII (1,000 ng/kg/min, H-1705, Bachem) was infused via a subcutaneously implanted osmotic pump (either Alzet model 2001 for 3 days for experiments using aortic tissues prior to overt pathology, or model 2004 for 28 days, Durect) into male mice at 10 to 14 weeks of age, as described previously.[17] Surgical staples were used to close incision sites and were removed 7 days after surgery. Post-operative pain was alleviated by application of topical lidocaine cream (4% wt/wt, LMX4, #0496-0882-15, Eloquest Healthcare, Inc).

*Aortic tissue proteolysis for mass spectrometry assisted proteomics:*

Aortic tissues harvested after 3 days of either saline or AngII infusion were minced before submersion in RIPA buffer (#9806, Cell Signaling Technology) supplemented with protease inhibitor cocktail (#P8340, Sigma-Aldrich). Tissue pieces were placed in a Precellys CK14 homogenizing tube with RIPA buffer and ceramic beads (1.4 mm; Bertin Instruments). Samples were homogenized on a Precellys 24 tissue homogenizer using three 10 second cycles at 5,000 rpm. Debris were removed by centrifugation for 10 minutes at 4°C and protein concentrations of supernatant samples were measured using the Pierce BCA Protein Assay (#23225, Thermo Fisher). Equal amounts of protein (10 µg) for each aortic segment were processed using the PreOmics iST in solution trypsinization kit (#00027, PreOmics) according to the manufacturer's recommended protocols. The final peptide precipitate was dissolved in sample buffer (40 µl, 5% wt/vol acetonitrile, 0.5% wt/vol formic acid in mass spectrometry grade water).

*Aortic cell suspension for single cell RNA sequencing (scRNAseq):*

Ascending aortic samples were harvested from Mef2c-*Cre* ROSA26R$^{mT/mG}$ male mice (n=5) and pooled in Hanks' Balanced Salt Solution (HBSS, #14175095, Thermo Fisher Scientific) with fetal bovine serum (10% vol/vol). Periaortic tissues were removed and aortic tissues were cut into small pieces. Aortic samples were subsequently digested with enzyme cocktail (**Supplemental Table II**) in Ca/Mg contained-HBSS (#14025092, Thermo Fisher Scientific) for 60 minutes at 37°C. Cell suspensions were filtered through a 40 μm cell strainer (CLS431750-50EA, Sigma-Aldrich), centrifuged at 300 g for 10 minutes, and resuspended using cold HBSS (#14175095) with fetal bovine serum (5% vol/vol). Cells were stained with DAPI and sorted to select viable cells (≥ 95% viability) by flow cytometry (FACS Aria III, BD Biosciences). Cells were also sorted based on mTomato and mGFP signals.

*scRNAseq:*

mTomato or mGFP positive cells were dispensed separately onto the Chromium Controller (10x Genomics) and indexed single cell libraries were constructed by a Chromium Single Cell 3' v2 Reagent Kit (10x Genomics). cDNA libraries were then sequenced in a pair-end fashion on an Illumina NovaSeq 6000. Raw FASTQ data were aligned to the mouse transcriptome (mm10) by Cell Ranger 3.0.

*Statistical analyses:*

Data are presented as the mean±standard error of the mean. Normality and homogeneity of variance were assessed by Shapiro-Wilk test and Brown-Forsythe test, respectively. Ascending aortic diameter data were log10 transformed to pass normality tests. After confirming homogeneous variances and normality, two-group and multi-

group comparisons for means were performed by two-sided Student's t-test or two-way analysis of variance (ANOVA) with Holm-Sidak multiple comparison test, respectively. The log-rank test was used to compare the probabilities of ascending aortic rupture between groups. In the log-rank test, deaths due to other causes such as abdominal aortic rupture were censored. $P<0.05$ was considered statistically significant. Statistical analyses mentioned above were performed using SigmaPlot version 14.0 (SYSTAT Software Inc.).

Statistical analyses for proteomics data were performed by Qlucore Omics Explorer 3.5 (Qlucore). For a principal component analysis (PCA) plot and heat maps, proteins were filtered by their false discovery rate adjusted P value (q-value) of two-group or multiple group comparisons with q=0.1 as a threshold. Proteins in the PCA plot were clustered by k-means algorithm (k=3). Protein-protein interaction networks were examined using the STRING database (version 11.0) in Cytoscape (version 3.8.0).[18] Interactions were acquired using the following thresholds: confidence interaction scores ≥0.150, active interaction sources = text mining, experiments, databases, co-expression, neighborhood, gene fusion, co-occurrence. Detected proteins were launched with either LRP1 or TGF-β signaling molecules cited from KEGG PATHWAY Database (#04350). Protein-protein interaction figures were modified using Photoshop CC 2019 (Adobe Systems Incorporated).

scRNAseq data analyses were performed using the Seurat package (version 3.1.4) on R (version 3.6.3).[19] Mapped unique molecular identifier (UMI) counts from mTomato and mGFP positive cells were imported into R separately. Seurat objects for each of the UMI count datasets were built using the "CreateSeuratObject" function by

the following criteria: >3 cells and >2,000 detected genes. Cells expressing less than 200 or more than 5,000 genes were filtered out for exclusion of non-cell or cell aggregates, respectively. Cells with more than 10% mitochondrial genes were also excluded. UMI counts were then normalized as the following: counts for each cell were divided by total counts, multiplied by 10,000, and transformed to natural-log. “FindIntegrationAnchors” function was used to integrate two normalized datasets and remove batch effects. Uniform manifold approximation and projection (UMAP) dimensionality reduction with PCA was applied to visualize cell clusters using the normalized- and scaled-UMI count data. “FindAllMarkers” and “FindConcervedMarkers” functions were used to identify conserved marker genes in each of the clusters. Differentially expressed genes were examined using “zinbwave” and “edgeR” packages with a negative binomial generalized log-linear model.[20, 21]

## Results

*Region-specific alteration of aortic protein profiles following AngII infusion.*

AngII was infused into C57BL/6J mice,[14] and ascending and descending aortic tissues were harvested after 3 days prior to development of overt pathology. Aortas from saline-infused mice were included as controls. Mass spectrometry-assisted proteomics was performed to investigate mechanisms driving regional specificity of TAAs. Proteomics analysis identified 2,644 proteins among all aortic samples. In principal component analyses using the unfiltered proteome, protein profiles of ascending and descending aortas in saline-infused mice were not significantly different. However, AngII infusion altered these profiles compared to saline infusion, and profiles were significantly different between ascending and descending thoracic regions (40% variation along PC1, **Figure 1A**). In the ascending aorta, AngII infusion differentially regulated 864 protein abundances compared to the saline-infused group (**Figure 1B**). Within AngII-infused mice, abundances of 77 proteins were different between ascending and descending aortas (**Figure 1B**). Forty two proteins were common between these two subsets, indicating that these molecules may be specific targets for TAA formation (**Figure 1B, C**). Previous studies demonstrated that LRP1, a multi-functional protein expressed in SMCs, contributed to aortic wall integrity, with deletion of LRP1 in pan SMCs leading to TAA formation in mice.[22-25] Thus, protein-protein interactions of LRP1 and 42 overlapped molecules were analyzed usingSTRING.[18] LRP1 had a direct interaction with 10 proteins including several LRP1 ligands: plasminogen activator inhibitor 1 (PAI1), thrombospondin 1, and matrix metalloproteinase 2 (**Figure 1D**). Although aortic LRP1 protein abundance was not changed by AngII (**Figure 1E**), AngII

altered the abundance of these ligands in the ascending aorta (**Figure 1F**).

*Susceptibility of SHF-derived cells to AngII-induced medial pathology.*

We next examined interactions between SMC origins and AngII-induced aortic pathology. CNC- and SHF-derived cells were tracked using Wnt1- or Mef2c-*Cre* ROSA26R$^{LacZ}$ mice infused with AngII. Consistent with our previous study,[13] the ascending aorta was composed of both CNC- and SHF-derived SMCs with neither extending beyond the distal boundaries of the aortic arch (**Figure 2A**). AngII increased medial area, while it did not alter distribution of SMC origins (**Figure 2B, C**). Of interest, X-gal positive areas were increased significantly in SHF-, but not CNC-, derived cells (**Figure 2D**). These data support that AngII induces medial thickening in both CNC- and SHF-derived cells, but SHF-derived cells may be more susceptible to AngII-induced medial thickening. These data are consistent with SHF-derived SMCs exerting a critical role in AngII-induced aortic pathologies.

*Differential gene expression between SHF- and CNC-derived SMCs*

To investigate cell-specific differences between SHF- and CNC-derived SMCs, scRNAseq was performed using Mef2c-*Cre* ROSA26R$^{mT/mG}$ male mice (n=5, **Supplemental Figure IA**). Aortic samples were harvested from the ascending region and suspended aortic cells were sorted by FACS based on mTomato and mGFP signals (**Supplemental Figure IA**, mTomato=13,549 cells, mGFP=17,573 cells). Since mGFP protein was expressed in Mef2c-*Cre* expressing cells of this mouse strain, mGFP positive cells were derived from the SHF; while, mTomato positive cells were derived from the other origins (nSHF, **Figure 3A**, **C**). scRNAseq detected gene expression in 22,571 cells of multiple cell types (**Figure 3B**, **Supplemental Figure IB, C**). SHF-

derived cells were composed of 37% SMCs (**Supplemental Figure ID**). Because SMCs in the ascending aorta are derived from either the SHF or CNC, nSHF-SMCs were considered as CNC-derived cells (**Figure 3C**). In the SMC cluster, 2,262 genes were expressed differentially between SHF- and CNC-SMC (up- and downregulated in SHF: 1,996 and 266 genes, respectively, **Supplemental Excel File**, **Supplemental Figure IE**). mRNAs related to SMC contractile proteins were more abundant in SHF-derived SMCs than in CNC-derived SMCs (**Figure 3D**). Several collagen genes including collagen type 1a1, 1a2, 3a1, and 5a2 were expressed differentially between SMC origins (**Figure 3E**). It is notable that elastin, a major component of the aortic media, was significantly less abundant in SHF-derived SMCs compared to CNC-derived SMCs (**Figure 3E**). Interestingly, TGF-β ligands such as *Tgfb2* and *3* were upregulated in SHF-derived SMCs compared to CNC-derived SMCs (**Figure 3F**). In addition, *Lrp1 and TGF-β receptor 2* were highly abundant in SHF-derived SMCs (**Figure 3F**).

*Augmentation of thoracic aortopathies by LRP1 deletion in SHF-derived cells.*

Deletion of LRP1 in all SMCs causes multiple aortic pathologies including aneurysm and tortuosity,[22-24] but it is unclear whether LRP1 deletion in a specific SMC lineage affects TAA formation. Therefore, we deleted LRP1 in either CNC- or SHF-derived SMCs. Mice with CNC-specific deletion of LRP1 using the Wnt1 promoter to drive *Cre* expression were embryonically lethal between E11.5 and E12.5 (**Supplemental Figure IIA**). Gross appearances of fetuses were comparable between genotypes at E11.5 with no obvious vascular malformation (**Supplemental Figure IIB**). Since this promoter is not restricted to the aorta (**Supplemental Figure III**), extra-aortic LRP1 deletion may have contributed to the embryonic lethality. Next, LRP1 was deleted

in SHF-derived SMCs using a Mef2c promoter driven *Cre*. In Mef2c-*Cre*-expressing mice, *Cre* activity was observed mainly in the outer media (**Supplemental Figure IVA**). *Lrp1 delta flox* fragment was observed in addition to a band of native *Lrp1* (**Supplemental Figure IVB-D**). LRP1 protein abundance was reduced by 37% in the ascending aortic media of SHF-specific LRP1 deleted mice compared to *Cre* negative littermates, and LRP1 deletion was restricted in the outer media (**Supplemental Figure IVE-F**). SHF-specific LRP1 deletion did not affect growth or development of mice. To promote TAAs, AngII was infused subcutaneously for 4 weeks. LRP1 deletion in SHF-derived cells augmented AngII-induced aortic dilation in the ascending aorta as demonstrated by both ultrasound and confirmed by in situ imaging (**Figure 4A, B**). Aortic pathology was not observed in the descending thoracic aorta (**Figure 4A**). SHF-specific LRP1 deletion also exacerbated AngII-induced ascending aortic rupture and elastin fragmentation (**Figure 4C-E**). Systolic blood pressure was not different between genotypes in response to AngII infusion (**Figure 4F**), demonstrating that augmented aortopathy was independent of systolic blood pressure. To explore molecular mechanisms behind augmentation of TAAs by LRP1 deletion in SHF-derived cells, proteomics analyses were performed using aortas harvested from wild type and SHF-specific LRP1 deleted mice. Analyses were performed under basal conditions and after a brief interval of AngII infusion that did not cause overt pathology. Deletion of LRP1 in SHF-derived cells was verified by the reduction of peptide intensity in the ascending aorta of Mef2c-*Cre* expressing mice (**Supplemental Figure V**). Based on $q<0.1$ threshold, deletion of LRP1 in SHF-derived cells altered abundances of seven proteins (**Figure 4G**). Of note, protein-protein interaction analysis using the STRING database

revealed that six of these proteins were associated with TGF-β signaling molecules (**Figure 4H**). In addition to LRP1, LTBP2, Col12a1, and CRYAB had a direct link to TGF-β ligands and receptors. These results indicate that the protective function of LRP1 in SHF-derived SMCs against AngII-induced TAA associates with alterations of TGF-β signaling-related proteins.

*Prenatal thoracic aortopathy induced by TGF-β receptor 2 deletion in SHF-derived cells.*

Genetic mutations of *TGFBR2* cause Loeys-Dietz syndrome (LDS) with probands predisposed to aneurysms.[26-28] In mice, postnatal deletion of TGFBR2 in SMCs promotes severe TAA formation with pathologies localized to outer medial layers of the ascending aorta.[9, 29] Since regional and transmural location of pathologies in LDS corresponded to distribution of SHF-derived SMCs, we investigated the role of TGFBR2 in SHF-derived cells on aortic structure. SHF-specific TGFBR2 depletion led to embryonic lethality with retroperitoneal hemorrhage beginning at E12.5 (**Figure 5A**). In addition, the outflow tract was dilated significantly in fetuses with SHF-specific TGFBR2 deletion compared to wild type littermates (**Figure 5A, B**). These data, alongside our findings in SHF-derived LRP1, support the premise that SHF-derived SMCs exert a critical role in the structural integrity and aneurysm development in the ascending aorta.

## Discussion

Our study demonstrated that AngII infusion induced region-specific alterations of protein profiles in the thoracic aorta and that SHF-derived cells were susceptible to AngII-induced medial pathology. scRNAseq revealed gene alterations related to extracellular matrix and TGF-β signaling in SHF-derived SMCs. Gene manipulation studies using mice with SHF-specific *Lrp1* or *Tgfbr2* deletion demonstrated that SHF-specific SMCs exerts an important role in the pathophysiology of thoracic aortopathies.

Our proteomic analysis identified 42 target proteins that were altered by AngII infusion and exhibited different abundances between aortic regions in wild type mice. Multiple studies including our previous report showed protective effects of LRP1 in the pathophysiology of aortic diseases.[22-25, 30-33] In addition, a previous in vitro study reported an increase of LRP1 abundance in SMCs incubated with AngII.[34] Thus, we focused on LRP1 to investigate the effects of these 42 proteins on aortic integrity. Despite significant aortic dilatation after AngII infusion, aortic LRP1 abundance was not increased in either the ascending or descending thoracic region in the present study. However, the identified 42 proteins included some extracellular matrix proteinase-related proteins such as plasminogen activator inhibitor 1, thrombospondin 1, and matrix metalloproteinase 2. These molecules have been implicated in medial disruption and aneurysm formation.[35-37] Of interest, LRP1 plays a pivotal role in extracellular removal of these molecules by functioning as an endocytic receptor,[30] and these molecules are increased in aneurysmal aortas.[23, 36] Therefore, LRP1 may contribute to AngII-induced aortopathies through increases in extracellular proteinases.

Elastin fragmentation is a pathological feature of TAAs and is associated with

decrease of aortic resilience.[38, 39] As elastin fibers are one of the major aortic components and are vital for maintaining aortic structure,[40] mutations of the elastin gene causes aortic stenosis due to overgrowth of SMCs.[38, 39] Also, SMC-specific elastin deletion induces TAA formation in mice.[41] Therefore, decreased elastin synthesis contributes to aortopathy formation. Our scRNAseq data revealed lower abundance of elastin in SHF-derived SMCs compared to CNC-derived SMCs in normal mouse aortas. Furthermore, TGF-β signaling molecules, including its ligands and receptors, were increased in SHF-derived SMCs. This may explain the basis for the outer medial layers derived from the SHF being susceptible to aortic pathologies. Because our proteomic analysis showed that AngII infusion changed the protein profile including extracellular matrix proteinases prior to TAA formation, further scRNAseq studies using AngII-infused aortas are needed to examine whether gene profiles related to extracellular matrix including elastin exhibit differential responses to AngII between SMC origins.

A number of studies have shown an important role for TGF-β signaling in maintaining aortic wall integrity.[9, 26-28] Both LRP1 and TGFBR2 are related to TGF-β signaling pathways,[26, 30] and genetic deletions of these molecules in pan-SMCs promotes TAA formation in mice.[9, 10, 22-24, 29] The present study demonstrated promotion of thoracic aortopathy by deletion of these proteins only in SHF-derived cells. These data are consistent with the outer layers of SMC derived from the SHF being crucial for development of thoracic aortopathies related to TGF-β signaling. A recent study using mice expressing a fibrillin1 mutation (*Fbn1*$^{C1041G/+}$) reported that heterozygous deletion of Notch1 in SHF-derived cells had a trend for augmenting luminal dilatation of the aortic sinus.[42] In contrast, another recent study demonstrated that Smad2 deletion in

CNC-derived cells reduced dilation of the aortic sinus in a mouse model of LDS.[43] Since there are aortic region-specific responses to TGF-β,[44] these two developmental origins may have divergent pathophysiological functions in different aortic regions.

In the present study, LRP1 deletion in CNC-derived cells did not lead to vascular malformation during the prenatal phase, but this manipulation led to embryonic lethality. Previous studies have reported that prenatal deletion of TGFBR2 in CNC-derived cells results in cleft palate and a congenital heart defect, persistent truncus arteriosus.[45, 46] These mice die in the immediate postnatal period. Therefore, the postnatal effects of LRP1 and TGFBR2 in CNC-specific cells are unknown. Because the Wnt1 gene is not expressed in the postpartum phase,[47] mouse experiments using inducible gene deletion are not feasible. Developments of research methods are needed to overcome this barrier to compare the role of two different SMC origins on formation of thoracic aortopathies.

In conclusion, our study highlights the functional importance of SHF-derived cells in maintaining the integrity of the ascending aortic wall using multiple TAA mouse models. This study provides strong evidence that SHF-derived cells exert a protective role during the development of TAA. Heterogeneity of SMC origins contributes to complex mechanisms of TAA formation, which should be taken into consideration when investigating the pathophysiology of TAAs.

**Acknowledgment**

Study design: HS, HH, CZ, YL, SM, SAS, JZC, DLR, HSL, YHS, MA, MWM, AD.

Implementation of animal experiments: HS, CZ, JJM, DAH, DLR.

Data analyses: HS, YK, DLR, HSL, AD.

Proteomics and associated informatics: HS, HH, SM, LHL, SAS.

scRNAseq and associated informatics: HS, YK, CZ, YL, YHS.

Supervising and data verification: YHS, SAL, MA, MWM, AD.

Writing and editing the manuscript: all authors.

**Sources of Funding**

The authors' research work was supported by the National Heart, Lung, and Blood Institute of the National Institutes of Health [R01HL133723 (AD), R01HL126901 (MA), R01HL149302 (MA), R01HL121877 (MWM)] and the American Heart Association SFRN in Vascular Disease (18SFRN33960163 and 33960114). HS was supported by an AHA postdoctoral fellowship (18POST33990468). JZC was supported by NCATS UL1TR001998 and NHLBI F30HL143943. SAL is supported in part by the Jimmy and Roberta Howell Professorship in Cardiovascular Surgery at Baylor College of Medicine. The content in this manuscript is solely the responsibility of the authors and does not necessarily represent the official views of the National Institutes of Health.

**Disclosures**

The following authors have declared that no conflict of interest exists: HS, CZ, YL, YK, SM, LHL, SAS, JZC, JJM, DAH, DLR, HSL, YHS, SAL, MA, MWM, AD. HH is an

employee of Kowa Company, Ltd. (Nagoya, Japan) and was a visiting scientist at Brigham and Women's Hospital when the study was conducted.

**Supplemental Materials**

Supplemental Methods

Supplemental Table I – V

Supplemental Figure I – V

Supplemental Excel File

## References


1. Goldfinger JZ, Halperin JL, Marin ML, Stewart AS, Eagle KA and Fuster V. Thoracic aortic aneurysm and dissection. *J Am Coll Cardiol*. 2014;64:1725-1739.
2. Hiratzka LF, Bakris GL, Beckman JA*, et al.* 2010 ACCF/AHA/AATS/ACR/ASA/SCA/SCAI/SIR/STS/SVM Guidelines for the diagnosis and management of patients with thoracic aortic disease. A Report of the American College of Cardiology Foundation/American Heart Association Task Force on Practice Guidelines, American Association for Thoracic Surgery, American College of Radiology,American Stroke Association, Society of Cardiovascular Anesthesiologists, Society for Cardiovascular Angiography and Interventions, Society of Interventional Radiology, Society of Thoracic Surgeons,and Society for Vascular Medicine. *J Am Coll Cardiol*. 2010;55:e27-e129.
3. Isselbacher EM. Thoracic and abdominal aortic aneurysms. *Circulation*. 2005;111:816-828.
4. Albornoz G, Coady MA, Roberts M, Davies RR, Tranquilli M, Rizzo JA and Elefteriades JA. Familial thoracic aortic aneurysms and dissections--incidence, modes of inheritance, and phenotypic patterns. *Ann Thorac Surg*. 2006;82:1400-1405.
5. Trachet B, Piersigilli A, Fraga-Silva RA, Aslanidou L, Sordet-Dessimoz J, Astolfo A, Stampanoni MF, Segers P and Stergiopulos N. Ascending aortic aneurysm in angiotensin II-infused mice: Formation, progression, and the role of focal dissections. *Arterioscler Thromb Vasc Biol*. 2016;36:673-681.

6. Daugherty A, Rateri DL, Charo IF, Owens AP, Howatt DA and Cassis LA. Angiotensin II infusion promotes ascending aortic aneurysms: attenuation by CCR2 deficiency in apoE-/- mice. *Clin Sci (Lond)*. 2010;118:681-689.
7. Wanga S, Hibender S, Ridwan Y*, et al.* Aortic microcalcification is associated with elastin fragmentation in Marfan syndrome. *J Pathol*. 2017;243:294-306.
8. Sawada H, Chen JZ, Wright BC, Sheppard MB, Lu HS and Daugherty A. Heterogeneity of aortic smooth muscle cells: A determinant for regional characteristics of thoracic aortic aneurysms? *J Transl Int Med*. 2018;6:93-96.
9. Li W, Li Q, Jiao Y, Qin L, Ali R, Zhou J, Ferruzzi J, Kim RW, Geirsson A, Dietz HC, Offermanns S, Humphrey JD and Tellides G. Tgfbr2 disruption in postnatal smooth muscle impairs aortic wall homeostasis. *J Clin Invest*. 2014;124:755-767.
10. Yang P, Schmit BM, Fu C, DeSart K, Oh SP, Berceli SA and Jiang Z. Smooth muscle cell-specific Tgfbr1 deficiency promotes aortic aneurysm formation by stimulating multiple signaling events. *Sci Rep*. 2016;6:35444.
11. Quintana RA and Taylor WR. Cellular mechanisms of aortic aneurysm formation. *Circ Res*. 2019;124:607-618.
12. Majesky MW. Developmental basis of vascular smooth muscle diversity. *Arterioscler Thromb Vasc Biol*. 2007;27:1248-1258.
13. Sawada H, Rateri DL, Moorleghen JJ, Majesky MW and Daugherty A. Smooth muscle cells derived from second heart field and cardiac neural crest reside in spatially distinct domains in the media of the ascending aorta-Brief report. *Arterioscler Thromb Vasc Biol*. 2017;37:1722-1726.

14. Rateri DL, Davis FM, Balakrishnan A, Howatt DA, Moorleghen JJ, O'Connor WN, Charnigo R, Cassis LA and Daugherty A. Angiotensin II induces region-specific medial disruption during evolution of ascending aortic aneurysms. *Am J Pathol*. 2014;184:2586-2595.
15. Owens AP, 3rd, Subramanian V, Moorleghen JJ, Guo Z, McNamara CA, Cassis LA and Daugherty A. Angiotensin II induces a region-specific hyperplasia of the ascending aorta through regulation of inhibitor of differentiation 3. *Circ Res*. 2010;106:611-619.
16. Robinet P, Milewicz DM, Cassis LA, Leeper NJ, Lu HS and Smith JD. Consideration of sex differences in design and reporting of experimental arterial pathology studies-statement from ATVB council. *Arterioscler Thromb Vasc Biol*. 2018;38:292-303.
17. Lu H, Howatt DA, Balakrishnan A, Moorleghen JJ, Rateri DL, Cassis LA and Daugherty A. Subcutaneous angiotensin II infusion using osmotic pumps induces aortic aneurysms in mice. *J Vis Exp*. 2015:10.3791/53191.
18. Szklarczyk D, Gable AL, Lyon D, Junge A, Wyder S, Huerta-Cepas J, Simonovic M, Doncheva NT, Morris JH, Bork P, Jensen LJ and Mering CV. STRING v11: protein-protein association networks with increased coverage, supporting functional discovery in genome-wide experimental datasets. *Nucleic Acids Res*. 2019;47:D607-D613.
19. Butler A, Hoffman P, Smibert P, Papalexi E and Satija R. Integrating single-cell transcriptomic data across different conditions, technologies, and species. *Nat Biotechnol*. 2018;36:411-420.

20. Risso D, Perraudeau F, Gribkova S, Dudoit S and Vert JP. A general and flexible method for signal extraction from single-cell RNA-seq data. *Nat Commun*. 2018;9:284.
21. Robinson MD, McCarthy DJ and Smyth GK. edgeR: a Bioconductor package for differential expression analysis of digital gene expression data. *Bioinformatics*. 2010;26:139-140.
22. Boucher P, Gotthardt M, Li WP, Anderson RG and Herz J. LRP: role in vascular wall integrity and protection from atherosclerosis. *Science*. 2003;300:329-332.
23. Davis FM, Rateri DL, Balakrishnan A, Howatt DA, Strickland DK, Muratoglu SC, Haggerty CM, Fornwalt BK, Cassis LA and Daugherty A. Smooth muscle cell deletion of low-density lipoprotein receptor-related protein 1 augments angiotensin II-induced superior mesenteric arterial and ascending aortic aneurysms. *Arterioscler Thromb Vasc Biol*. 2015;35:155-162.
24. Basford JE, Koch S, Anjak A, Singh VP, Krause EG, Robbins N, Weintraub NL, Hui DY and Rubinstein J. Smooth muscle LDL receptor-related protein-1 deletion induces aortic insufficiency and promotes vascular cardiomyopathy in mice. *PLoS One*. 2013;8:e82026.
25. Muratoglu SC, Belgrave S, Hampton B, Migliorini M, Coksaygan T, Chen L, Mikhailenko I and Strickland DK. LRP1 protects the vasculature by regulating levels of connective tissue growth factor and HtrA1. *Arterioscler Thromb Vasc Biol*. 2013;33:2137-2146.
26. Lindsay ME and Dietz HC. Lessons on the pathogenesis of aneurysm from heritable conditions. *Nature*. 2011;473:308-316.

27. Schmit BM, Yang P, Fu C, DeSart K, Berceli SA and Jiang Z. Hypertension overrides the protective effect of female hormones on the development of aortic aneurysm secondary to Alk5 deficiency via ERK activation. *Am J Physiol Heart Circ Physiol*. 2015;308:H115-125.
28. Gallo EM, Loch DC, Habashi JP*, et al.* Angiotensin II-dependent TGF-beta signaling contributes to Loeys-Dietz syndrome vascular pathogenesis. *J Clin Invest*. 2014;124:448-460.
29. Hu JH, Wei H, Jaffe M, Airhart N, Du L, Angelov SN, Yan J, Allen JK, Kang I, Wight TN, Fox K, Smith A, Enstrom R and Dichek DA. Postnatal deletion of the type II transforming growth factor-beta receptor in smooth muscle cells causes severe aortopathy in mice. *Arterioscler Thromb Vasc Biol*. 2015;35:2647-2656.
30. Strickland DK, Au DT, Cunfer P and Muratoglu SC. Low-density lipoprotein receptor-related protein-1: role in the regulation of vascular integrity. *Arterioscler Thromb Vasc Biol*. 2014;34:487-498.
31. Llorente-Cortes V and Badimon L. LDL receptor-related protein and the vascular wall: implications for atherothrombosis. *Arterioscler Thromb Vasc Biol*. 2005;25:497-504.
32. Boucher P, Li WP, Matz RL, Takayama Y, Auwerx J, Anderson RG and Herz J. LRP1 functions as an atheroprotective integrator of TGFbeta and PDFG signals in the vascular wall: implications for Marfan syndrome. *PLoS One*. 2007;2:e448.
33. Bown MJ, Jones GT, Harrison SC*, et al.* Abdominal aortic aneurysm is associated with a variant in low-density lipoprotein receptor-related protein 1. *Am J Hum Genet*. 2011;89:619-627.

34. Sendra J, Llorente-Cortes V, Costales P, Huesca-Gomez C and Badimon L. Angiotensin II upregulates LDL receptor-related protein (LRP1) expression in the vascular wall: a new pro-atherogenic mechanism of hypertension. *Cardiovasc Res*. 2008;78:581-589.
35. Allaire E, Hasenstab D, Kenagy RD, Starcher B, Clowes MM and Clowes AW. Prevention of aneurysm development and rupture by local overexpression of plasminogen activator inhibitor-1. *Circulation*. 1998;98:249-255.
36. Yamashiro Y, Thang BQ, Shin SJ, Lino CA, Nakamura T, Kim J, Sugiyama K, Tokunaga C, Sakamoto H, Osaka M, Davis EC, Wagenseil JE, Hiramatsu Y and Yanagisawa H. Role of thrombospondin-1 in mechanotransduction and development of thoracic aortic aneurysm in mouse and humans. *Circ Res*. 2018;123:660-672.
37. Shen M, Lee J, Basu R, Sakamuri SS, Wang X, Fan D and Kassiri Z. Divergent roles of matrix metalloproteinase 2 in pathogenesis of thoracic aortic aneurysm. *Arterioscler Thromb Vasc Biol*. 2015;35:888-898.
38. Li DY, Brooke B, Davis EC, Mecham RP, Sorensen LK, Boak BB, Eichwald E and Keating MT. Elastin is an essential determinant of arterial morphogenesis. *Nature*. 1998;393:276-280.
39. Curran ME, Atkinson DL, Ewart AK, Morris CA, Leppert MF and Keating MT. The elastin gene is disrupted by a translocation associated with supravalvular aortic stenosis. *Cell*. 1993;73:159-168.
40. Shen YH and LeMaire SA. Molecular pathogenesis of genetic and sporadic aortic aneurysms and dissections. *Curr Probl Surg*. 2017;54:95-155.

41. Lin CJ, Staiculescu MC, Hawes JZ, Cocciolone AJ, Hunkins BM, Roth RA, Lin CY, Mecham RP and Wagenseil JE. Heterogeneous cellular contributions to elastic laminae formation in arterial wall development. *Circ Res*. 2019;125:1006-1018.
42. Koenig SN, LaHaye S, Feller JD, Rowland P, Hor KN, Trask AJ, Janssen PM, Radtke F, Lilly B and Garg V. Notch1 haploinsufficiency causes ascending aortic aneurysms in mice. *JCI Insight*. 2017;2:10.1172/jci.insight.91353.
43. MacFarlane EG, Parker SJ, Shin JY*, et al.* Lineage-specific events underlie aortic root aneurysm pathogenesis in Loeys-Dietz syndrome. *J Clin Invest*. 2019;129:659-675.
44. Topouzis S and Majesky MW. Smooth muscle lineage diversity in the chick embryo. Two types of aortic smooth muscle cell differ in growth and receptor-mediated transcriptional responses to transforming growth factor-beta. *Dev Biol*. 1996;178:430-445.
45. Ito Y, Yeo JY, Chytil A, Han J, Bringas P, Jr., Nakajima A, Shuler CF, Moses HL and Chai Y. Conditional inactivation of Tgfbr2 in cranial neural crest causes cleft palate and calvaria defects. *Development*. 2003;130:5269-5280.
46. Choudhary B, Ito Y, Makita T, Sasaki T, Chai Y and Sucov HM. Cardiovascular malformations with normal smooth muscle differentiation in neural crest-specific type II TGFbeta receptor (Tgfbr2) mutant mice. *Dev Biol*. 2006;289:420-429.
47. Echelard Y, Vassileva G and McMahon AP. Cis-acting regulatory sequences governing Wnt-1 expression in the developing mouse CNS. *Development*. 1994;120:2213-2224.

## References for Supplemental Methods


1. Rateri DL, Davis FM, Balakrishnan A, Howatt DA, Moorleghen JJ, O'Connor WN, Charnigo R, Cassis LA and Daugherty A. Angiotensin II induces region-specific medial disruption during evolution of ascending aortic aneurysms. Am J Pathol. 2014;184:2586-2595.

2. Sawada H, Chen JZ, Wright BC, Moorleghen JJ, Lu HS and Daugherty A. Ultrasound imaging of the thoracic and abdominal aorta in mice to determine aneurysm dimensions. J Vis Exp. 2019:10.3791/59013.

3. Chen JZ, Sawada H, Moorleghen JJ, Weiland M, Daugherty A and Sheppard MB. Aortic strain correlates with elastin fragmentation in fibrillin-1 hypomorphic mice. Circ Rep. 2019;1:199-205.

4. Daugherty A, Rateri D, Hong L and Balakrishnan A. Measuring blood pressure in mice using volume pressure recording, a tail-cuff method. J Vis Exp. 2009:10.3791/1291.

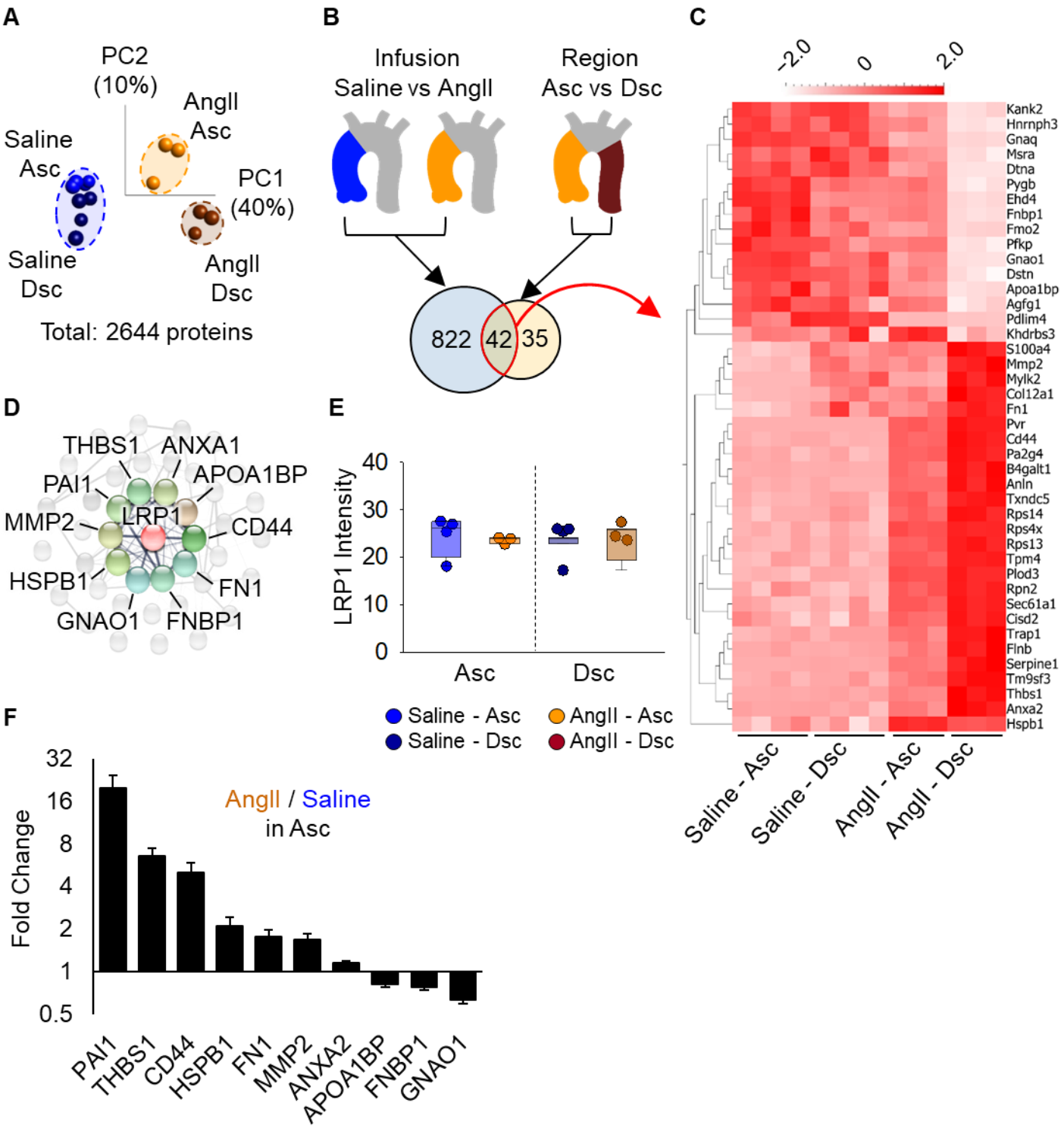


**Figure 1. AngII differentially altered the protein profile of ascending and descending aortas of LRP1 ligands. (A)** Principal component analysis of the unfiltered proteome. Asc indicates ascending aorta; and Dsc, descending aorta (n=3 to

4 per group). **(B)** Venn diagram of differentiated proteins (q<0.1). **(C)** Heat map with Z score coloring for overlapped 42 proteins. **(D)** Protein-protein interaction between overlapped 42 proteins and LRP1. **(E)** Aortic LRP1 peptide intensity. **(F)** Fold change of protein intensity related to LRP1 in overlapped 42 proteins by comparing AngII- vs saline-infused mice.

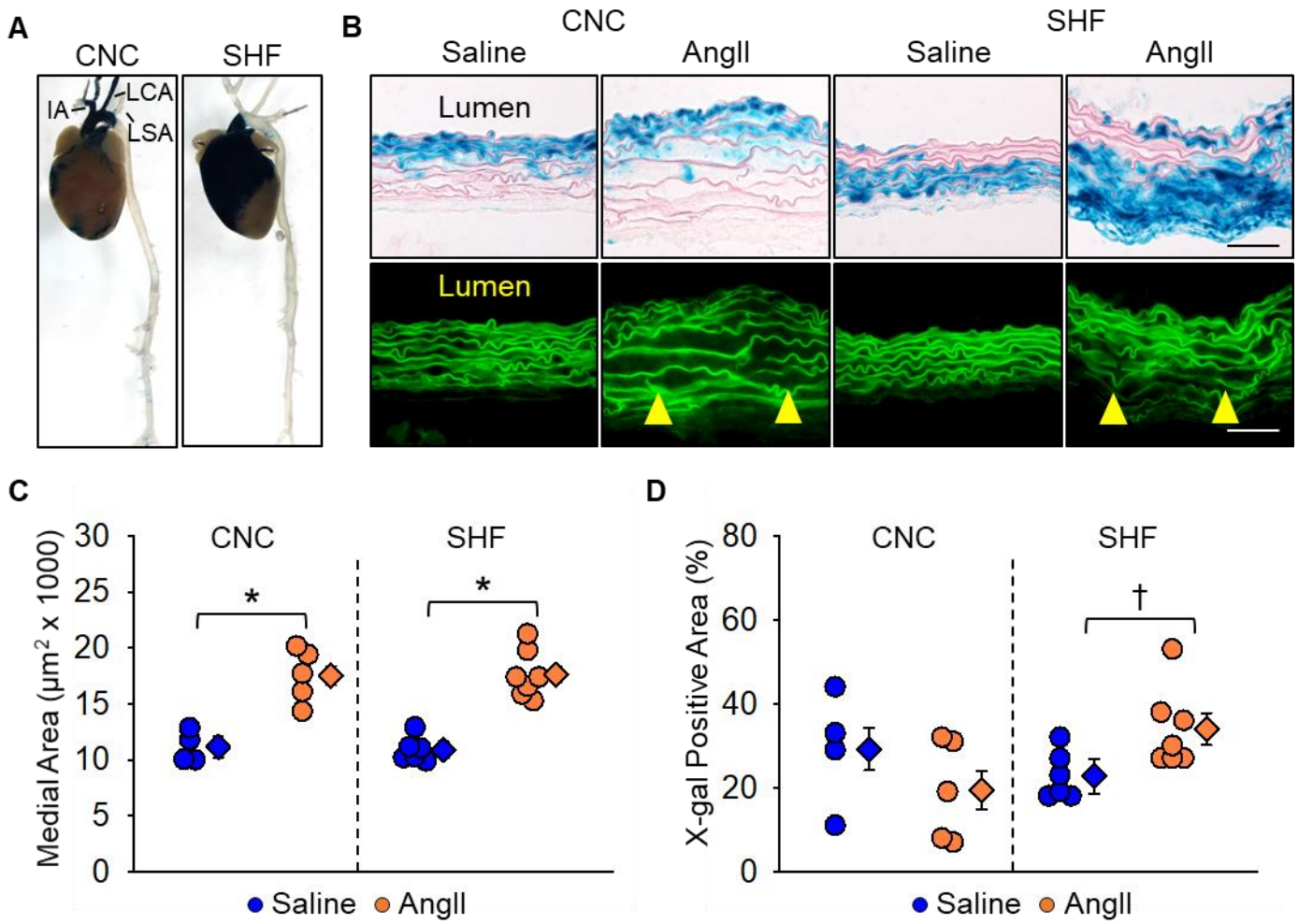


**Figure 2. AngII-induced medial disruption was predominantly in outer medial layers derived from the SHF. (A)** Representative images of X-gal stained aortas from Wnt1- and Mef2c-*Cre* ROSA26R$^{LacZ}$ mice (n=3 per group). IA indicates innominate artery; LCA, left common carotid artery; and LSA, left subclavian artery. **(B)** Representative X-gal staining and FITC images of aortas from either saline- or AngII-infused Wnt1- and Mef2c-*Cre* ROSA26R$^{LacZ}$ mice (n=5 to 7 per group). Yellow triangles indicate medial thickening. Scale bar, 50 µm. Dot plots for **(C)** medial area and **(D)** X-gal positive area in the media. *P<0.001, †P<0.05 by two-way ANOVA followed by Holm-Sidak test.

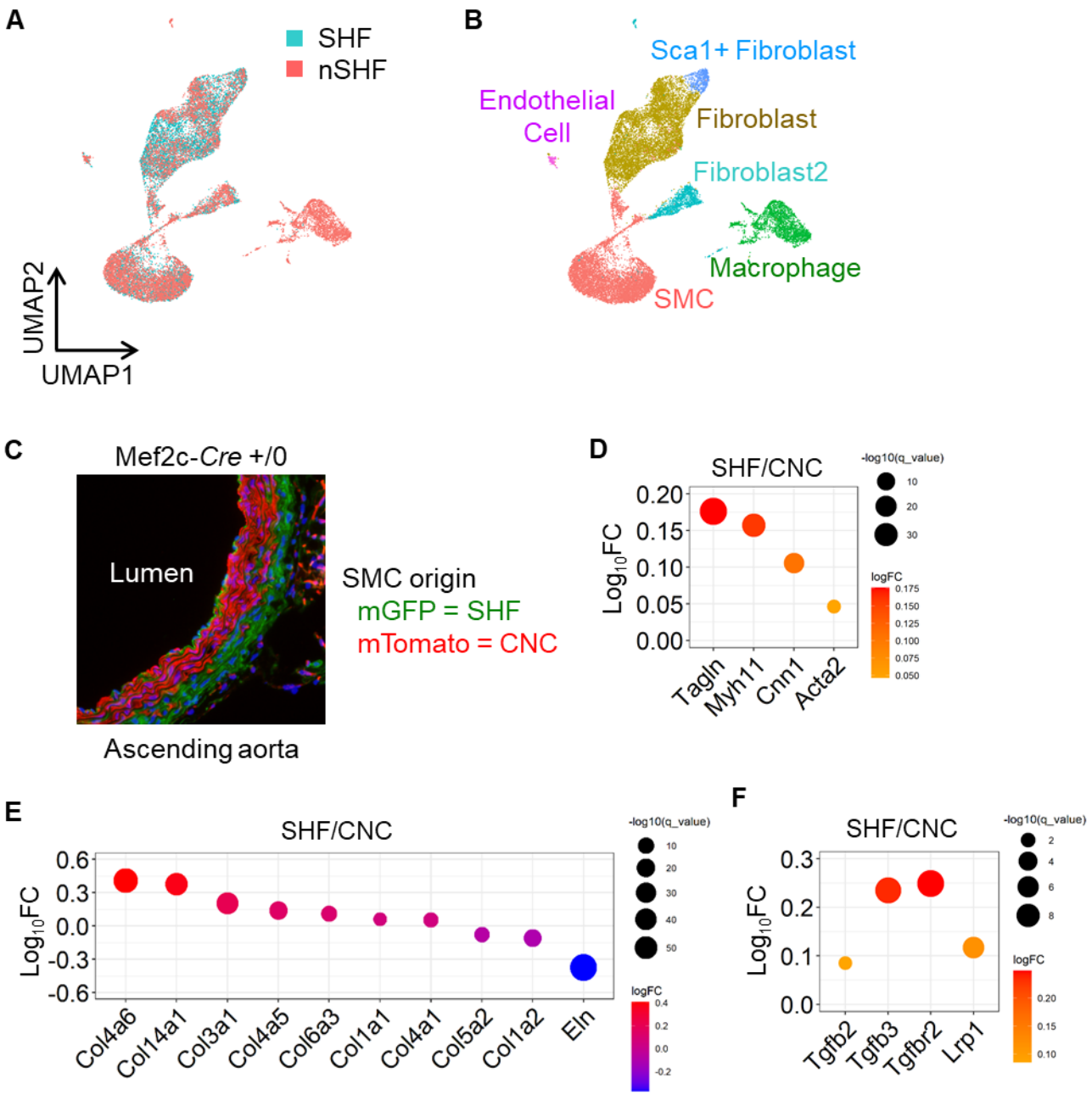


**Figure 3. SHF-derived SMCs exhibited differential mRNA abundance related to extracellular matrix components and TGF-β ligands and receptors. (A)** UAMP plot of aortic cells in scRNAseq using Mef2c-Cre ROSA26RmT/mG mice (n=5). Colors denote mGFP (derived from the SHF) and mTomato (not derived from the SHF, nSHF) positive cells. **(B)** Renamed UAMP plot including six cell types: SMC, fibroblasts, fibroblast 2, Sca1+ fibroblasts, endothelial cells, and macrophages. **(C)** Representative

cross-sectional image of the aorta from Mef2c-*Cre* +/0 ROSA26R$^{mT/mG}$ mice. Fold change (SHF/CNC) of genes related to **(D)** SMC contractility, **(E)** collagen and elastin fibers, and **(F)** TGF-β ligands and receptors.

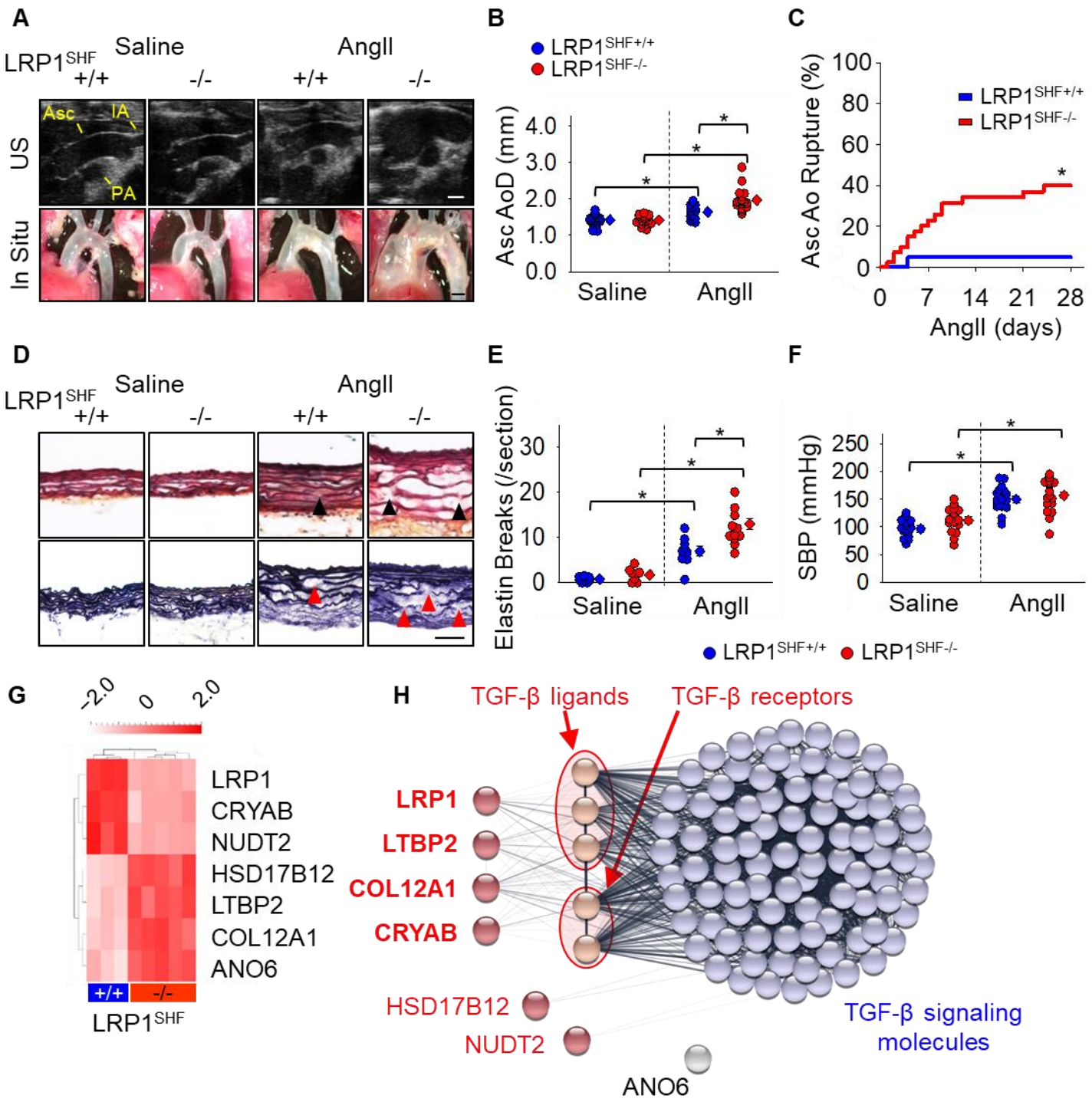


**Figure 4. LRP1 deletion in SHF-derived SMCs augmented AngII-induced TAA formation and aortic rupture. (A)** Representative ultrasound (US) images and in situ gross appearances of proximal thoracic aortas. n=21 to 40 per group. Asc indicates

ascending aorta; IA, innominate artery; and PA, pulmonary artery. Scale bar, 1 mm. **(B)** Ascending aortic diameter measured by ultrasonography. **(C)** Probability of ascending aortic rupture. **(D)** Representative Movat's and Verhoeff iron hematoxylin staining. Scale bar, 50 µm. **(E)** Elastin break counts in Movat's stained sections. **(F)** Systolic blood pressure. **(G)** Heat map with Z score coloring for differentiated proteins in comparison between wild type and SHF-specific LRP1 deleted ascending aortas ($q<0.1$, $n=3$ to 5 per group). **(H)** Protein-protein interaction between 7 identified proteins and TGF-β signaling molecules. Proteins in red font had a link to TGF-β signaling molecules.
*$P<0.001$ by two-way ANOVA followed by Holm-Sidak test, or Log rank test.

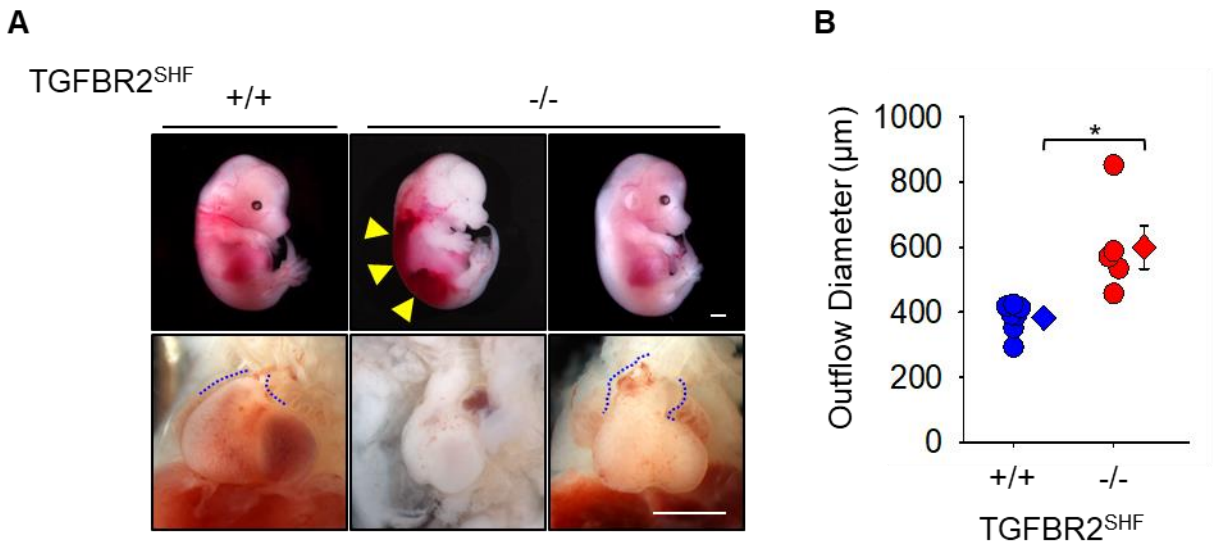


**Figure 5. TGF-β receptor 2 deletion in SHF-derived cells provoked embryonic lethality and thoracic aortopathy at the embryonic stage. (A)** Representative images of gross appearance and outflow tract of wild type littermates (left), dead (middle), and survived (right) fetuses with SHF-specific TGFBR2 deletion at E12.5. Blue dotted lines indicate the edge of the outflow tract. **(B)** Outflow diameter was measured at 300 to 400 μm distal to the root of fetuses that survived at the termination. n=5 to 7 per group. Yellow triangles indicate retroperitoneal hemorrhage. Scale bar, 1 mm. *P<0.001 by two-tailed Student's t test.